Renewable Energy 66 (2014) 425–432

Contents lists available at ScienceDirect

Renewable Energy

journal homepage: www.elsevier.com/locate/renene

Hydraulic impacts of hydrokinetic devices

Maria Kartezhnikova*, Thomas M. Ravens

Department of Civil Engineering, University of Alaska Anchorage, 3211 Providence Drive, Anchorage, AK 99508, USA

ARTICLE INFO

Article history:
Received 9 April 2013
Accepted 27 December 2013
Available online 23 January 2014

Keywords:
Hydrokinetic energy
In-stream hydrokinetic turbines
Hydraulic impacts
Rivers
Manning roughness

ABSTRACT

A simple technique to estimate the far-field hydraulic impacts associated with the deployment of hydrokinetic devices is introduced. The technique involves representing hydrokinetic devices with an enhanced Manning (bottom) roughness coefficient. The enhanced Manning roughness is found to be a function of the Manning roughness, slope, and water depth of the natural channel as well as device efficiency, blockage ratio, and density of device deployment. The technique is developed assuming simple open channel flow geometry. However, once the effective bottom roughness is determined, it can be used to determine the hydraulic impact of arbitrary device configurations and arbitrary flow situations.

1. Introduction

The kinetic energy of flowing water, or hydrokinetic energy, is a large potential source of renewable energy [12,17]. Hydrokinetic energy conversion devices are deployed in flowing water, and they extract energy according to the kinetic energy or velocity of the flowing water. The power available from hydrokinetic devices, per unit swept area, is termed the hydrokinetic power density (PD, W/m^2). Hydrokinetic power density is a function of fluid velocity (V, m/s), fluid density (ρ, kg/m^3), and device efficiency (ξ):

$$\mathrm{PD} = \xi \frac{\rho}{2} V^3 \tag{1}$$

However, as hydrokinetic (HK) devices extract power from flowing water, they can alter the flow velocity, water elevation, sediment transport and other river properties/processes. The goal of this paper is to present a simple way of estimating and representing the far-field hydraulic impacts of HK device deployments. In particular, a technique for representing the presence of hydrokinetic devices with an enhanced bottom roughness is developed. The enhanced bottom roughness can be used in standard hydraulic calculation procedures and models to determine the device impact.

A widely-used open channel flow equation for relating flow velocity (or discharge) to bottom roughness and channel properties is the Manning Equation. Here, the equation is presented in two forms:

$$V = \frac{1}{n} R^{2/3} S^{1/2} \quad \text{or} \quad Q = \frac{A}{n} R^{2/3} S^{1/2} \tag{2}$$

where V = cross-section averaged velocity (m/s); n = Manning roughness coefficient (s/m$^{1/3}$); R = hydraulic radius (cross-sectional area/wetted perimeter, m); S = slope; Q = discharge (m^3/s); and A = cross-sectional area (m^2).

Note, the second version of the Manning Equation is obtained from the first through application of the continuity principle ($Q = VA$). Since HK devices tend to impede the flow of water, they can be represented with an enhanced bottom roughness, n_t. According to the Manning equation, all other parameters being unchanged, an enhanced bottom roughness would cause a reduction in velocity. In a river setting, where the discharge can be considered constant, the reduced velocity will be compensated for with an increase in water depth.

The majority of previous research on the interaction of HK devices and flowing water focused on the calculation of the available HK power in tidal systems [4,5,9,10,15,20]. In tidal systems, often conceptualized as a channel connecting two basins [6] – one semi-infinite and one finite – the central question is: what fraction of the total energy passing through the tidal channel is available for HK extraction? The researchers found that as the number of HK devices increased, the flow rate of water through the channel decreased. Further, as the number of devices increased, there was a peak in total energy extraction followed by a decline.

Researchers [19] have also addressed the question of the relationship between the power extracted by hydrokinetic devices

* Corresponding author.
E-mail address: mekartuozhnikova@alaska.edu (M. Kartezhnikova).

0960-1481
http://dx.doi.org/10.1016/j.renene.2013.12.034

($P_{extracted}$) and the total power dissipated by the presence of the devices ($P_{dissipated}$). The power extracted by hydrokinetic devices is the product of the power density (PD) and the swept area of the devices. Focusing on a single device in a channel, Garrett and Cummins [8] and Polagye [19] noted that the devices generated a low velocity zone in their wake. Further, when the low water velocity wake mixed with the high velocity water that flowed around the device, significant energy was dissipated. Polagye concluded that with a turbine operating at the efficiency close to maximum theoretical limit, the ratio of power extraction ($P_{extracted}$) to power dissipation ($P_{dissipated}$) can be approximated as follows:

$$\frac{P_{extracted}}{P_{dissipated}} = \frac{2}{3(1+\varepsilon)} \tag{3}$$

where ε = blockage coefficient (i.e., the fraction of the river cross-sectional area occupied by the HK device); and $P_{dissipated}$ is the total power dissipated in a river stretch due to the presence of the devices. $P_{dissipated}$ includes the extracted power and additional dissipation due to mixing. It is assumed that there are negligible drag losses.

Here, we derive an expression for an enhanced or effective Manning roughness coefficient (n_t) that can be used to represent the presence of hydrokinetic devices. The expression is obtained by considering the conservation of energy equation in two simple flow situations – case A and case B. Case A is a wide open channel flow situation in which the flow is steady and uniform. In case B, hydrokinetic devices have been deployed such that they are distributed uniformly throughout the channel bottom. The channel in case B is otherwise identical to the one in case A. Assuming that the total flow rate is the same in both situations, an expression for an enhanced Manning roughness that accounts for the presence of devices is readily determined.

In a river deployment of hydrokinetic devices, it is reasonable to assume that the flow rate will be largely unchanged by the presence of devices. Rivers are water conveyance systems for transporting water from high in the watershed to lower in the watershed. However, in parallel with river flow, some amount of water will be transported (from higher to lower in the watershed) in the form of groundwater flow. Neglecting changes in storage, which would be transient, the total flow rate will be unaffected by the deployment of hydrokinetic devices, due to the conservation of mass principle. The build-up of river water upstream of a large deployment of devices could potentially shift some of the downward flow from river flow to groundwater flow. However, the shift would normally be relatively small because the resistance to flow of underground water is extremely large compared to the resistance to flow of surface water. Hence, it is reasonable to assume that the flow rate is the same in case A and B.

2. Representation of hydrokinetic devices with an enhanced bottom roughness

2.1. Case A – uniform open channel flow with no hydrokinetic devices

Assuming flow from location 1 to location 2, the energy conservation equation (or modified Bernoulli Equation) for case A (no devices) can be written [18]:

$$\frac{P_1}{\gamma} + \frac{V_1^2}{2g} + z_1 = \frac{P_2}{\gamma} + \frac{V_2^2}{2g} + z_2 + h_L \tag{4}$$

where P_1 and P_2 = pressure (Pa) at locations 1 and 2, respectively; V_1 and V_2 = velocity (m/s) at locations 1 and 2, respectively; z_1 and z_2 = elevations (m) at locations 1 and 2, respectively; γ = specific weight (N/m^3); g = acceleration due to gravity (9.8 m/s^2); and h_L = head loss (m) due to bottom friction.

Since flow is uniform in the direction of flow, the pressure and velocity terms cancel out and the energy equation can be written:

$$z_1 - z_2 = \Delta z = h_L \tag{5}$$

Further, recognizing that, for uniform flow, the bottom slope is the ratio of the head loss to the length of the channel section (i.e., $S = h_L/L$), Manning's Equation (Eq. (2)) can be rearranged to obtain head loss in terms of the flow rate, Manning's roughness, channel cross section area (A, m^2), and hydraulic radius (R, m):

$$h_L = \Delta z = \left(\frac{Qn}{AR^{2/3}}\right)^2 L \tag{6}$$

2.2. Case B – uniform open channel flow with uniform distribution of hydrokinetic devices

In case B, the channel of case A is altered to include hydrokinetic devices (i.e., turbines) that are distributed uniformly on the channel bottom. Water pressure (P_{1t} and P_{2t}) and flow velocity (V_{1t} and V_{2t}) differ from that seen in case A due to the presence of the devices. However, variables such as discharge, channel width, and bottom slope remain the same. The energy conservation equation for case B has the following form:

$$\frac{P_{1t}}{\gamma} + \frac{V_{1t}^2}{2g} + z_1 = \frac{P_{2t}}{\gamma} + \frac{V_{2t}^2}{2g} + z_2 + h_{Lt} + h_p \tag{7}$$

where h_{Lt} = head loss due to the bottom friction (i.e., contact of the flowing water with the "natural" channel bottom); and h_p = "head loss" associated with the presence of the hydrokinetic devices (described below).

Since the turbines are uniformly distributed, flow conditions continue to be uniform in the direction of flow. Consequently, upstream and downstream velocity and pressure heads are the same and Eq. (7) can be simplified to:

$$z_1 - z_2 = \Delta z = h_{Lt} + h_p \tag{8}$$

Consideration of Eqs. (5) and (8), for case A and B, respectively, allows one to readily see that the addition of a uniform distribution of hydrokinetic devices in a river segment leaves the total energy loss in the segment unchanged. However, while the energy loss (head loss) is attributable entirely to bottom friction in case A (without devices), in case B (with devices) the head loss has a contribution due to bottom friction and a contribution due to hydrokinetic devices. Essentially, shifting from case A to B, the natural energy dissipation is reduced to exactly compensate for the increase dissipation from turbines.

Using the same approach as for Eq. (5), the head loss associated with bottom friction can be expressed:

$$h_{Lt} = \left(\frac{Qn}{A_t R_t^{2/3}}\right)^2 L \tag{9}$$

where A_t and R_t are the cross-sectional area and hydraulic radius of the channel when turbines are present.

Since the channel geometry in the two cases is the same, Eq. (8) can be written using Eqs. (6)–(9) obtaining:

$$\left(\frac{Qn}{AR^{2/3}}\right)^2 L = \left(\frac{Qn}{A_t R_t^{2/3}}\right)^2 L + h_p \tag{10}$$

Assuming a very wide rectangular channel such that the hydraulic radius is the water depth and the cross-sectional area is the product of the width and depth, Eq. (10) becomes:

$$\left(\frac{Qn}{wh^{5/3}}\right)^2 L - \left(\frac{Qn}{wh_t^{5/3}}\right)^2 L - h_p = 0 \tag{11}$$

where h = water depth without HK devices (m); h_t = water depth with devices present (m).

2.3. Channel energy losses due to presence of hydrokinetic devices

Assuming drag losses to be negligible following [19], the total power dissipated can be estimated based on the blockage area and extracted power as described in Eq. (3). The total power dissipated can be expressed as a "head loss" (i.e., as h_p) by dividing by the product of discharge and the specific weight (i.e., $\gamma \cdot Q$) obtaining:

$$h_p = \frac{P_{dissipation}}{\gamma Q} = \frac{3}{4}\frac{\rho N A_r V_t^3}{\gamma Q}(\xi(1+\varepsilon)) = \left(\frac{3}{4}\frac{N A_r Q^2}{g w^3}\cdot\xi(1+\varepsilon)\right)\cdot\frac{1}{h_t^3} \tag{12}$$

where N = number of hydrokinetic devices in the channel segment; A_r = swept area of an individual hydrokinetic device (m^2); V_t = cross-section averaged velocity with devices present (m/s); w = channel width (m); and h_t = channel depth with devices present (m).

This approach for estimating head loss due to HK device operation probably works best for devices with high efficiencies; since ratio of power extracted to power dissipated (Eq. (3)) was derived for high efficiency devices.

2.4. Determination of water depth with devices present

Using the expression for "head loss" due to the presence of hydrokinetic devices (Eq. (12)), Eq. (11) can be rearranged obtaining:

$$h^{-10/3} - h_t^{-10/3} - \left(\frac{3}{4}\frac{\xi(1+\varepsilon)}{n^2 g}\cdot\frac{N A_r}{wL}\right)\cdot h_t^{-3} = 0 \tag{13}$$

From Eq. (13), it is apparent that the increased depth associated with the deployment of the hydrokinetic devices (h_t) can be determined from the character of the channel and the character and number of the devices. Through the principle of continuity, the cross-section averaged velocity could also be determined.

Eq. 13 was normalized by multiplying the entire equation by $h_t^{10/3}$, then the last term of equation is multiplied and divided by $h^{1/3}$, obtaining:

$$\left(\frac{h_t}{h}\right)^{10/3} - 1 - \left(\frac{3}{4}\frac{\xi(1+\varepsilon)}{n^2 g}\cdot\frac{N A_r}{wL}\right)\cdot h^{1/3}\cdot\left(\frac{h_t}{h}\right)^{1/3} = 0 \tag{14}$$

Following additional algebraic manipulations, Eq. (14) was converted to:

$$x^3 - x^{-1/3} - a = 0 \tag{15}$$

where: $x = \frac{h_t}{h}$, $a = \left(\frac{3}{4}\frac{\xi(1+\varepsilon)}{n^2 g}\cdot\frac{N A_r}{wL}\right)\cdot h^{1/3}$

Assuming, one is interested in modeling hydrokinetic device deployments which cause a water level rise of no more than 100% (relative to the depth of the natural channel), the variable x will range from 1 to 2, and variable a will range from 0 to 7.2063 (based on Eq. (15)). A cubic approximation was applied to Eq. (15) within the limits defined above, in order to eliminate fractional exponent in the second term, obtaining:

$$x^3 - x^{-1/3} - a \approx 1.0849\cdot x^3 - 0.45336\cdot x^2 + 0.98303\cdot x - 1.6145 - a = 0 \tag{16}$$

Knowing that x is a non-negative real integer, the expression for x is attainable from solving the cubic polynomial in Eq. (16). The solution was used to determine the following relationship between h_t, h, and a:

$$h_t = h\cdot\left(b - \frac{0.245}{b} + 0.0994\right) \tag{17}$$

where:

$$b = \left(0.4766\cdot a + \left((0.4766\cdot a + 0.69555)^2 + 0.01466\right)^{1/2}\right)^{1/3} + 0.69555$$

$$a = \left(\frac{3}{4}\frac{\xi(1+\varepsilon)}{n^2 g}\cdot\frac{N A_r}{wL}\right)\cdot h^{\frac{1}{3}}$$

For values of x ranging from 1 to 2 and for a ranging 0–7.2063, the cubic polynomial approximation was found to generate estimates of x (or h_t/h) that were very accurate (within 10^{-2} percent). Eq. (17) demonstrates that the hydraulic impacts of a uniform distribution of hydrokinetic devices can be estimated based on a single parameter, a.

Note, the solution presented in Eq. (17) is implicit since parameter a is a function of blockage ratio (ε) and, therefore, a function of h_t. As mentioned earlier, the blockage ratio is the fraction of the river cross-sectional area occupied by the HK devices. So, as water depth (h_t) increases with the number of the deployed HK devices, blockage ratio changes as well. In order to account for this change in depth, an iterative approach for estimation of representative blockage ratio is recommended. It was found that blockage ratio and consequently solution of Eq. (17) converge fairly quickly and two or three iterations are enough. However, for relatively small HK device deployment densities, one can forgo the iteration procedure and still have accurate calculations.

2.5. Determination of the effective Manning's roughness coefficient and velocity with devices present

Having determined h_t/h as a function of parameter a, the enhanced Manning roughness coefficient representing the presence of the hydrokinetic devices (i.e., turbines) can be readily determined. Since the discharge and slope under case A and B are the same, the Manning Equation, Eq. (2), can be used to establish a relationship between h_t, h, n and n_t:

$$\frac{wh}{n}h^{2/3} = \frac{wh_t}{n_t}(h_t)^{2/3} \tag{18}$$

Solving for n_t, we have:

$$n_t = \left(\frac{h_t}{h}\right)^{5/3} n \tag{19}$$

Based on the continuity principle, the velocity with devices present (V_t, m/s) can also be determined based on h_t/h or n_t/n:

$$V_t = \left(\frac{h}{h_t}\right)V = \left(\frac{n}{n_t}\right)^{3/5} V \tag{20}$$

2.6. Investigation of formulas

Eq. (11) can be solved using Eq. (6) for the altered water depth (h_t) as a function of the head loss due to the presence of HK devices (h_p):

$$h_t = h \cdot \left(1 - \frac{h_p}{\Delta z}\right)^{-3/10} \tag{21}$$

Substituting the altered water depth in Eq. (19), using Eq. (21), one obtains:

$$n_t = n \cdot \left(1 - \frac{h_p}{\Delta z}\right)^{-1/2} \tag{22}$$

The head loss due to the HK device presence as well as bottom friction (h_p) are functions of number of HK devices, as shown in Eq. (15). Applying Eqs. (21) and (22) for case A, when $N = 0$, conditions remain unchanged and $h_t = h$, $n_t = n$.

It is interesting to notice that $h_p < \Delta z$, since energy that can be extracted from the flow of water is always less than the total energy available. Therefore, for any $h_p \neq 0$ (case B), water depth (h_t, Eq. (21)) and effective Manning's roughness (n_t, Eq. (22)) attributed to device placement will exceed the case A parameters ($h_t > h$, $n_t > n$).

Therefore, HK devices will cause an increase in water depth and a decrease in velocity, assuming a uniform distribution of devices. Based on the derived equations, hydraulic impacts of HK devices can be estimated and modeled.

2.7. Example estimate of the hydraulic impacts of a uniform distribution of hydrokinetic devices

In order to illustrate the technique for estimating the hydraulic impact of hydrokinetic devices, a set of channel, flow, and hydrokinetic device properties were assumed (Table 1). Following the theoretical development presented above, it was assumed that HK devices were distributed uniformly over the channel bottom. In practice, devices are deployed in rows (perpendicular to the flow). The lateral distance between HK devices in a given row can be as small as 2–3 turbine diameters (D) [2,3]. The longitudinal spacing of the rows is larger due to persistence of the wake. Spacing between rows of the HK devices is recommended to be at least 10 D, since flow is significantly recovered at downstream distances of 10 D to 15 D [1,3,11].

The diameter of the devices was assumed to be 80 percent of the water depth (or 8 m) and longitudinal spacing of the rows was set to 10 D (or 80 m). For an increasing number of devices in the rows (i.e., the number of devices per 10 turbine diameters of channel length), the impact of the devices on the normalized depth (h_t/h), normalized effective bottom roughness (n_t/n), and normalized velocity (V_t/V) were calculated based on Eqs. (17, 19 and 20), respectively (Fig. 1). In this example, the maximum number of devices per row was capped at 18. This amounts to spacing between devices of 18.7 m or 2.3 D, which is approximately equal to upper density limit (2 D).

Table 1
Channel, flow, and turbine properties assumed in example calculation.

Variable	Symbol	Value
Water depth	h	10 m
Channel width	w	500 m
Slope	s	0.0002
Manning roughness	n	0.025
Turbine efficiency	ξ	32%
Turbine diameter	D	8 m

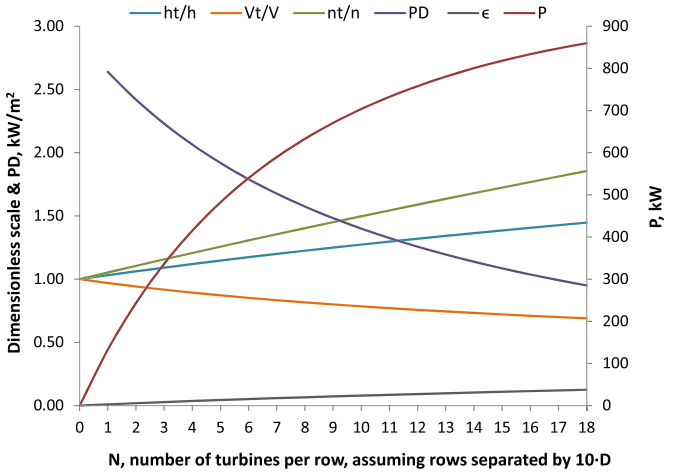

Fig. 1. Plot of normalized depth (h_t/h), normalized velocity (V_t/V), normalized effective Manning roughness (n_t/n), power density (PD, kW/m^2), and extracted power (P, kW) and blockage ratio (ε) as a function of density of hydrokinetic devices (number of devices per 10 D of channel length).

Fig. 1 also shows the blockage ratio (ε), power density, and total power extracted per row of hydrokinetic devices as a function of its density (i.e., number of devices per row). It is noteworthy that the normalized depth, Manning roughness, and velocity all start at a value of 1.0 on the left side of the plot (where the device density is 0). As the density of devices increases, the normalized depth and Manning roughness monotonically increase whereas the normalized velocity decreases. Initially, the total extracted power increases rapidly. Later, there are diminishing returns in extracted power with incremental increases of device density. This is because the water has been slowed by the devices that have already been deployed in the channel. The diminishing energy level of the channel with increasing device density is shown by the power density curve which decreases rapidly with increasing numbers of devices.

Note, the calculations presented in Fig. 1 are based on the implicit Eq. (17) and they reflect an iterative calculation scheme. If, for the case of 18 devices per row the iterative approach had been forgone, h_t would have increased by 1.2%.

3. Hydraulic impacts of HK devices associated with deployments in spatially limited areas

The analytical analysis for the uniform case provides the relationship between the character of the hydrokinetic device deployment and the level of effective bottom roughness enhancement. Once the appropriate level of bottom roughness enhancement is determined, it is valid to use that enhanced bottom roughness in a non-uniform numerical model, in the same way that one would use data on non-uniform spatial distribution of grain size (bottom roughness) in a non-uniform numerical model.

The previous section indicated that a uniform distribution of hydrokinetic devices can have a significant impact on water level and velocity. For example, with the conditions indicated in Table 1 and assuming that rows of devices are separated by 10 D (or 80 m), a deployment of 4.5 devices per row (i.e., alternating rows of 4 devices and 5 devices) would lead to a water level rise of about 1.3 m or about 13% of the original depth (Fig. 1). In order to determine the impact of hydrokinetic devices when they are deployed in limited areas, a 1D numerical model (ISIS) was employed.

ISIS (Halcrow Group Ltd.; http://www.halcrow.com/isis/) is a hydraulic model for determining depth-averaged velocity and

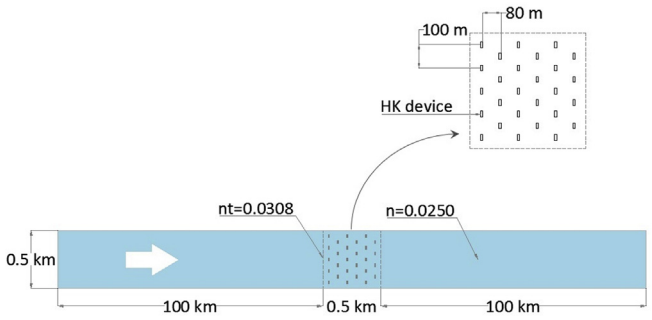

Fig. 2. Cartoon illustrating the spatially-limited deployment of hydrokinetic devices.

water level in open channels based on the St Venant equations derived from Navier–Stokes equations for steady flows [7]. Input to ISIS includes: the river profiles (or cross-section bathymetric/topographic data), spacing between profiles, river slope, and discharge. After verifying that ISIS produced calculations of velocity and water depth similar to the Manning Equation (within 1%) for channels with uniform distributions of devices (or no devices at all), ISIS was then used to determine the longitudinal distribution of water velocity and depth for situations in which the device deployment was limited to river segments of finite length. For simplicity, the same channel and device properties (Table 1), and the device density considered above (4.5 devices per row, one row every 10 D or 80 m) were used. A cartoon illustrating an example deployment (500-m long) is provided in Fig. 2. Note that a 100-km long, device-free, river segment was placed upstream and downstream of the devices to ensure that the hydraulic conditions on the boundaries were not affected by the presence of the devices. Based on the device density (rows separated by 10 D or 80 m and 4.5 devices per row), the effective Manning roughness (n_t) of the deployment area was calculated to be 0.0308 using Eqs. (17) and (19). Since the HK devices were distributed uniformly in rows, the density of the devices, $N/(Lw)$, could be calculated for the entire deployment area or for a single representative row. Adopting the latter approach, spacing between rows (10 D) was used for the L parameter and average density of the devices per row (4.5 devices) was used for the N parameter in Eq. (17).

The hydraulic impact of the 500-m long deployment is shown in Fig. 3. The figure indicates that the hydrokinetic device deployment "dams" the river water to some extent leading to maximal water levels just upstream of the deployment area. Water levels then fall with increasing longitudinal position within the device deployment area arriving at the device-free water level at the downstream end of the deployment area. Water levels are enhanced or equivalent to those of a device-free channel throughout. The longitudinal distribution of velocity follows directly from the depth distribution given the continuity equation. Velocity is reduced or equivalent to that of a device-free channel throughout. The minimum velocity is at the upstream edge of the deployment area.

The model results indicate that the 500-m long deployment had a significantly reduced hydraulic impact relative to the uniform deployment. For example, the 500-m deployment enhanced the maximum water depth by only about 0.06 m (Fig. 3). This increase in water depth is significantly less than the 1.3 m water depth increase when a uniform distribution of the same density is assumed. Thus, hydrokinetic device deployments in river segments of limited length have a limited hydraulic impact relative to the impact of a uniform distribution of the same density.

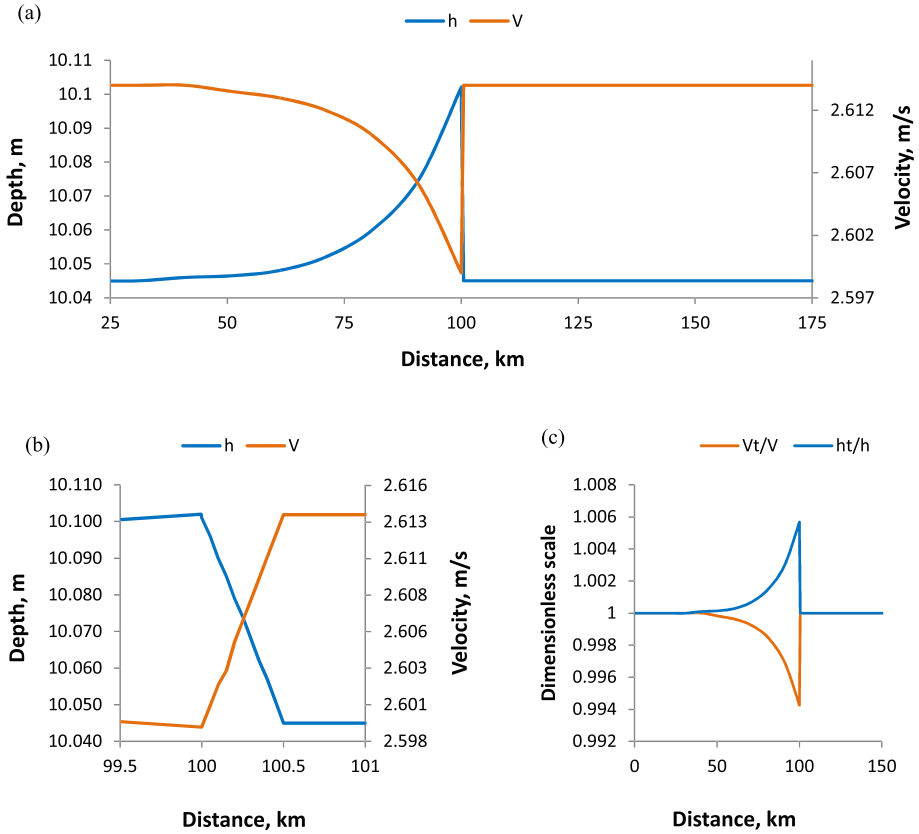

Fig. 3. Hydraulic impact of a spatially-limited deployment of hydrokinetic devices including: (a) velocity (V) and water depth (h) within 75 km of the hydrokinetic devices; (b) Velocity (V) and water depth (h) within 0.5 km of the devices; and (c) normalized velocity (V_t/V) and normalized depth (h_t/h) proximal to the devices.

The modeling described above for a 500-m long deployment area was extended to consider a range of deployment lengths from 0.5 to 150 km. In all cases, the segment with the hydrokinetic devices was preceded and followed by 100-km, device-free segments. Also, the same channel and device properties (Table 1) and device density (rows separated by 10 D or 80 m and 4.5 devices per row) was assumed. Plots of maximum dimensionless depth ($h_{t,max}/h$) and minimum dimensionless velocity ($V_{t,min}/V$) as a function of deployment length are provided in Fig. 4. The results show that when the deployment length reaches about 50 km, hydraulic impacts approach those of a uniform (i.e., infinitely long) deployment length.

4. Hydraulic impacts of a hypothetical deployment of hydrokinetic devices in the Kuskokwim River by Red Devil, Alaska

To illustrate the estimation of the far-field hydraulic impacts of a hypothetical deployment of hydrokinetic devices using the enhanced bottom roughness approach, the case of Red Devil on the Kuskokwim River in Alaska is presented. For this calculation, a 2-D hydraulic model, CCHE [21], was adopted. The CCHE flow model, which is based on the depth-averaged Navier–Stokes equations, determines the depth-averaged east and north velocity components as well as the water surface elevation. Inputs to the model include river bathymetry, topography, and discharge. In addition, in contrast to the 1-D ISIS model, a fixed water level boundary condition at the downstream boundary and a preliminary water level boundary condition at the upstream boundary are required for CCHE. These water levels were calculated using the Manning equation. The version of CCHE employed here used a two-dimensional k-ε model for the determination of the turbulent viscosity [21]. Fig. 5 depicts the calculated water depth and depth-averaged velocity (in the absence of HK devices) at a flow of 1956 m^3/s, which is the 50-percentile flow of the open water period (mid June–October) based on data from a nearby USGS gage.

It also indicates the location of a hypothetical deployment of HK devices, in a deep, high-velocity portion of the river. This deployment consisted of 18, 3-m diameter devices (Fig. 6). Based on the dimensions of deployment area, turbine characteristics, and device spacing (Fig. 6), the enhanced Manning roughness to represent the devices was estimated to be 0.039 (using Eqs. (17) and (19)). Summary information about the river segment and the deployment are provided in Table 2. Impacts of the deployment on velocity and depth are shown in Figs. 7 and 8, respectively.

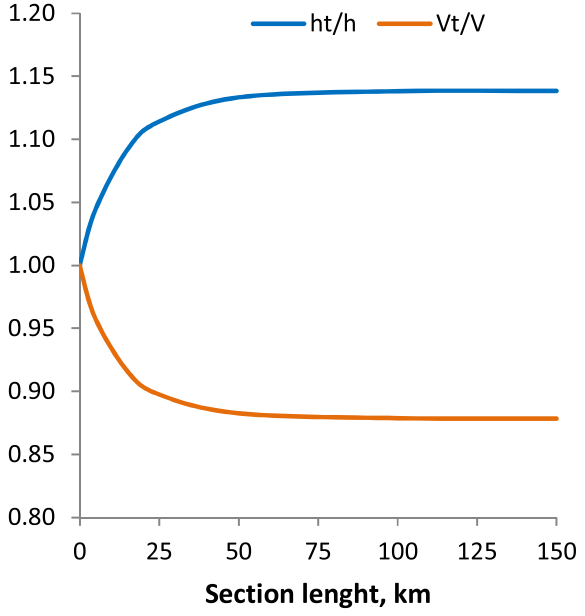

Fig. 4. Plot of maximum normalized depth ($h_{t,max}/h$) and minimum normalized velocity ($V_{t,min}/V$) as a function of section length with hydrokinetic devices.

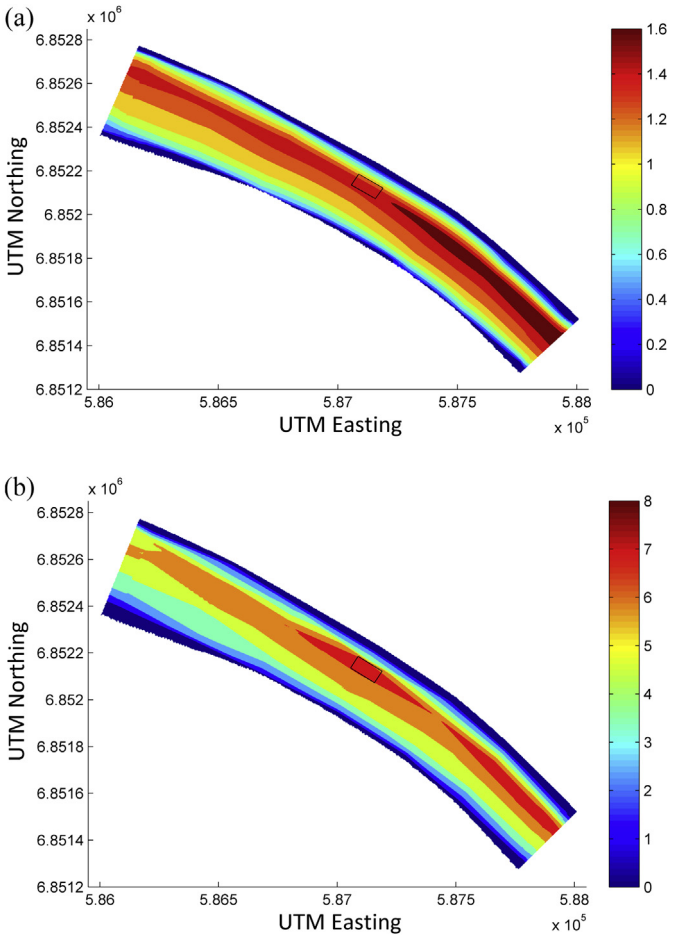

Fig. 5. (a) Plot of calculated water depth (m) at the 50-percentile flow (without hydrokinetic devices) and selected area for hydrokinetic devices deployment; (b) Plot of calculated depth-averaged velocity (m/s) at the 50-percentile flow.

Note, care was taken to ensure that the hydraulic impact of the devices was not felt at the upstream and downstream boundaries. Before running the CCHE model with the enhanced Manning roughness applied in the selected area (Fig. 5), a simplified 1-D rectangular channel model was created in ISIS using average characteristics of river channel. Results from the ISIS model, which adjusts the upstream and downstream boundary water level as appropriate, verified that device-impacts on the water level at the upstream and downstream ends were negligible (<0.3% change).

Fig. 7 demonstrates that velocity or momentum impacts of the deployment included velocity reduction (about −0.1 m/s) in the deployment area (where the Manning roughness coefficient had been enhanced), and velocity reduction downstream of the devices, i.e., in the wake of the devices. Laterally (in the cross-channel direction), the deployment caused an enhancement (+0.05 m/s) in velocity. Essentially, flow was diverted to the sides by the presence of the devices.

As with channel-wide HK device deployment (Fig. 3), placement of the HK devices led to an enhancement of water level upstream of the deployment area (up to approximately 1 cm), but little effect

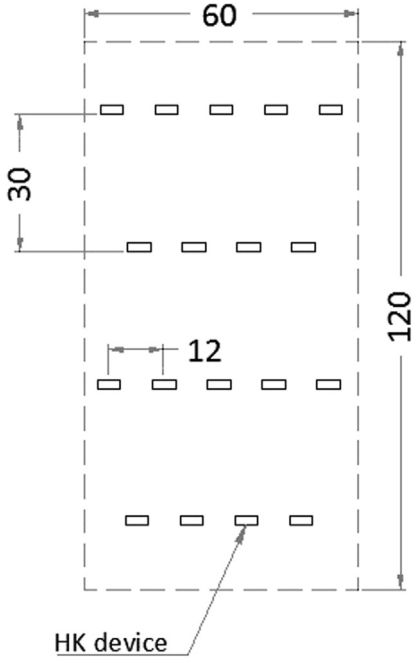

Fig. 6. Dimensions (m) of deployment area and spacing between HK devices.

downstream of the devices (Fig. 8). There was some noteworthy cross-channel variation in water depth in the vicinity of the deployment area.

Downstream wake effects persisted for almost 5 times the length of the deployment area (600 m). The length of the wake was probably over-predicted due to the inability of the effective Manning roughness approach to account for enhancement in turbulent kinetic energy and mixing associated with hydrokinetic energy extraction. The excessively long wake might also be attributed to the lateral mixing settings in CCHE, which in principle could be adjusted by the user.

The 18 hydrokinetic devices modeled would reduce the local velocity (at the 50-percentile flow) to 1.5 m/s and produce about 69 kW of power. The 69 kW was calculated based on device efficiency and swept area and based on the modeled velocity at the locations of the devices.

5. Discussion

The methodology described here can readily estimate the far-field impacts of hydrokinetic device deployments on water level, depth-averaged velocity, and related properties. For example, the calculation of velocity and water level change upstream and lateral

Table 2
Channel, flow, and turbine properties assumed.

Variable	Symbol	Value
Average water depth in deployment area at 50 percentile flow depth	h	7.5 m
Deployment width	w	60 m
Deployment length	L	120 m
River slope	S	0.000115
Manning roughness (without devices)	n	0.0257
Turbine efficiency	ξ	32%
Turbine diameter	D	3.0 m
Enhanced Manning roughness (4.5 turbines per row, 10 D spacing between rows)	n_t	0.0390

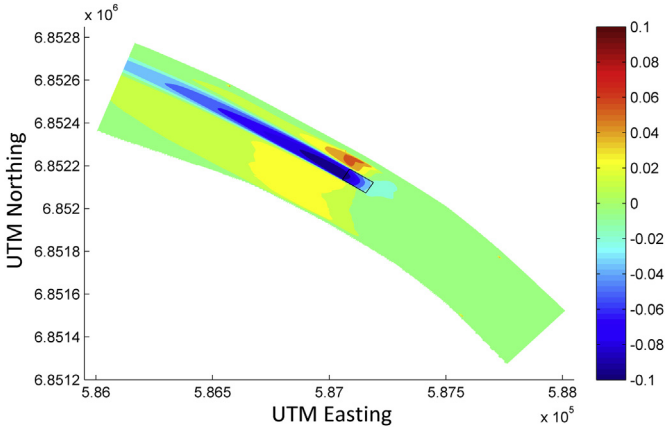

Fig. 7. Change in velocity distribution (m/s) due to the deployment of HK devices.

to the devices in the Red Devil example (Figs. 7 and 8) could be used to estimate the potential for sedimentation, scour, and bank erosion. As such, the methodology is a useful screening tool for estimating hydraulic and hydraulics-related impacts. However, the approach would not be able to determine fine-scale hydraulic impacts around individual devices. Further, since the approach is most directly applied in conjunction with depth-averaged hydraulic models, it cannot readily distinguish between a bottom-mounted and a surface-mounted device deployment. The approach focuses on the momentum-reducing aspect of HK devices. However, other researchers have noted that the devices enhance the turbulent kinetic energy and turbulent kinetic energy dissipation especially in their wake [13]. Detailed accounting of the wake behind devices would require an accounting for their impact on turbulent kinetic energy and mixing. For the case of modeling a single device with the described approach, enhanced bottom roughness can be applied on the rectangular area of 3D in the lateral direction and 10 D in the longitudinal direction at the area of the device deployment. Finally, some hydraulic models represent bottom roughness with parameters other than a Manning roughness coefficient. Simple equations relating the various bottom roughness parameters can be found in the literature [14,16]. Efforts are underway to validate the calculated hydraulic impacts with labs tests. Also, preliminary results indicated the hydraulic impacts calculated with the enhanced bottom roughness approach (described here) are in agreement with an alternative approach developed by Sandia National Laboratories.

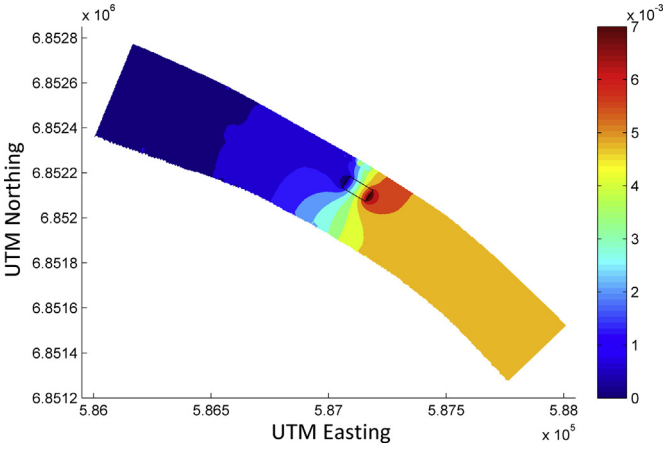

Fig. 8. Change in water depth (m) due to HK devices deployment.

6. Conclusion

A simple technique was developed to estimate the far-field hydraulic impacts of hydrokinetic devices using an enhanced Manning roughness coefficient. The approach would also enable an estimate of the maximum extractable energy. The enhanced Manning roughness was found to be a function of the Manning roughness, slope, and water depth of the natural channel as well as device efficiency, blockage ratio, and density of the device deployment. The approach was developed assuming a simple rectangular channel cross-section and a uniform distribution of devices. However, the enhanced bottom roughness concept can be applied for arbitrary device configurations and arbitrary flow situations. Here, the approach was applied to estimate the impacts of a number of example deployments. For device deployments in which devices could be considered to be uniformly distributed throughout a wide channel of uniform depth, increases in device density lead to uniform increases in water depth and uniform decreases in water velocity. Total energy extraction was observed to initially increase rapidly with increased device density. However, with subsequent device density increases there were marginal returns, as the power density decreased monotonically with increased device density. High device density leads to significant hydraulic impacts when the devices were uniformly distributed. However, when the devices (at a given density) were deployed in limited areas, the hydraulic impacts were significantly curtailed. The technique developed here would allow estimates of far-field hydrokinetic impacts to velocity, water surface elevation, and potential sediment transport. However, near-field hydraulic impacts around individual devices cannot be addressed with this technique. For example, the approach described here cannot distinguish between a bottom mounted and a surface mounted device.

Nomenclature

A	cross sectional area of the channel (m^2)
A_t	cross sectional area of the channel for the case when turbines are uniformly distributed over the bottom (m^2)
A_r	cross sectional area of the rotor for one turbine unit (m^2)
g	acceleration due to gravity (9.81 m/s)
h	water depth (m)
h_{Lt}	head loss due to bottom fiction the case when turbines are uniformly distributed over the bottom (m)
h_L	head loss due to bottom fiction (m)
h_p	head loss due to turbines operation, caused by power production and drag forces acting on the turbines (m)
h_t	water depth for the case when turbines are uniformly distributed over the bottom (m)
L	channel length (m)
$\dot{m}$	mass flow rate (kg/s)
n	Manning's roughness coefficient
n_t	effective Manning's roughness coefficient that is attributed to placing turbines
$P_{1,2}$	pressure at the point (N/m^2)
ρ	fluid density (1000 kg/m^3)
Q	volume flow rate (m^3/s)
R	hydraulic radius (m)
R_t	hydraulic radius for the case when turbines are uniformly distributed over the bottom (m)
S	slope of the channel (m/m)
V	average fluid flow velocity in the channel (m/s)
$V_{1,2}$	fluid flow velocity at a point on a streamline (m/s)
w	channel width (m)
$z_{1,2}$	elevation of the point above a reference plane (m)
Δz	elevation change over the channel length (m)
γ	specific weight (N/m^3)
ξ	turbine efficiency
ε	blockage ratio

References

[1] Bahaj A, Myers L, Thompson G. Characterising the wake of horizontal axis marine current turbines. In: Seventh European Wave and Tidal Energy Conference 2007. Ref type: Conference proceeding.

[2] Bai G, Li J, Fan P, Li G. Numerical investigations of the effects of different arrays on power extractions of horizontal axis tidal current turbines. Renew Energy 2013;53:180–6.

[3] Bai L, Spence R, Gudziak G. Investigation of the influence of array arrangement and spacing on tidal energy converter (TEC) performance using a 3-dimensional CFD model. In: 8th European Wave and Tidal Energy Conference 2009. Ref type: Conference proceeding.

[4] Blanchfield J, Garrett C, Wild P, Rowe A. The extractable power from a channel linking a bay to the open ocean. Proc IMechE Part A J Power Energy 2008;222:289–97.

[5] Bryden I, Couch S. ME1-marine energy extraction: tidal resource analysis. Renew Energy 2006;31:133–9.

[6] Couch S, Bryden I. The impact of energy extraction on tidal flow development. In: 3rd IMarEST International Conference on Marine Renewable Energy 2004.

[7] Evans E, Wicks J, Whitlow C, Ramsbottom D. The evolution of a river modelling system. Proc ICE Water Manag 2007;160:3–13.

[8] Garrett C, Cummins P. The efficiency of a turbine in a tidal channel. J Fluid Mech 2007;588:243–51.

[9] Garrett C, Cummins P. The power potential of tidal currents in channels. Proc Math Phys Eng Sci 2005;461:2563–72.

[10] Garrett C, Cummins P. Limits to tidal current power. Renew Energy 2008;33:2485–90.

[11] Gunawan B, Neary V, Hill C, Chamorro L. Measurement of velocity deficit at the downstream of a 1:10 axial hydrokinetic turbine model. In: Hydraulic measurements and experimental method 2012. Ref type: Conference proceeding.

[12] Jacobson P, Ravens T, Cunningham K, Scott G. Assessment and mapping of the riverine hydrokinetic resource in the continental United States; 2012. EPRI RP 1026880.

[13] James SC, Seetho E, Jones C, Roberts J. Simulating environmental changes due to marine hydrokinetic energy installations. In: OCEANS 2010 2010. pp. 1–10. Ref type: Conference proceeding.

[14] Julien PY. Erosion and sedimentation. Cambridge: Cambridge University Press; 2010.

[15] Karsten R, McMillan J, Lickley M, Haynes R. Assessment of tidal current energy in the Minas Passage, Bay of Fundy. Proc IMechE Part A J Power Energy 2008;222:493–507.

[16] Marriott MJ, Jayaratne R. Hydraulic roughness – links between Manning's coefficient, Nikuradse's equivalent sand roughness and bed grain size. In: Advances in Computing and Technology (AC&T), the School of Computing and Technology 5th Annual Conference. University of East London; 2010. pp. 27–32. Ref type: conference proceeding.

[17] Miller G, Franceschi J, Lese W, Rico J. The allocation of kinetic hydro energy conversion systems (KHECS) in USA drainage basins: regional resources and potential power; 1986. pp. 86–151. Report prepared for U. S. Department of Energy.

[18] Munson BR, Young DF, Okiishi TH. Fundamentals of fluid mechanics. Hoboken, NJ: John Wiley & Sons; 2006.

[19] Polagye B. Hydrodynamic effects of kinetic power extraction by in-stream tidal turbines. University of Washington; 2009. Ref type: Thesis/dissertation.

[20] Sutherland G, Foreman M, Garrett C. Tidal current energy assessment for Johnstone Strait, Vancouver Island. J Power Energy 2007;221:147–57.

[21] Zhang Y. CCHE2D-GUI – graphical users interface for NCCHE model. NCCHE-TR-2006-02. Oxford: University of Mississippi; 2006. Ref type: Report.